Electronic Supplementary Material (ESI) for Nanoscale.


# Supporting Information

# The implication of adsorption preferences of ions and surfactants on shape control of gold nanoparticles: a microscopic, atomistic perspective

Santosh Kumar Meena* and Chandrakala Meena

*Chemical Engineering and Process Development Division, CSIR-National Chemical Laboratory (NCL), Dr. HomiBhabha Road, Pune-411008, India*

E-mail: sk.meena@ncl.res.in

## Calculation of the surface densities on planar surfaces

The surface densities on planar were calculated as the number of ions present on the gold surface per unit area up to a 0.55 nm distance from the gold surface for $CTA^+$ and up to a 0.43 nm distance for $Br^-$. The same criteria as $Br^-$ was adopted For $Cl^-$ and $I^-$ for the planar surfaces. Detailed discussion about the cut-off used for these ions is provided in our previous work where the same criteria were used for ions adsorption studies on non-polarizable planar surfaces where.[1–3]

## Calculation of the surface densities on nanoseed

On the lateral facets of penta-twinned nanoseed particle, the surface density was evaluated by calculating the number of ions per unit area between the lateral surface and on outer pentagonal surface located at the cut-off distance (black line in Figure S3 top view). The surface density on the tip was calculated using the number of ions between surface parallel to the tip at the cut-off distance (the surface position is represented by the solid black line in Figure S3 side view) and the surface of the tip. A 0.55 nm cut-off was used for $CTA^+$ ions and a 0.43 nm distance cut-off was adopted for $Br^-$ and $Ag^+$ similar to our previous work on nano-polarizable nanoseeds and nanorods.[2] A 0.48 nm cut-off was used for $AuCl_2^-$ based on its equilibrium molecular length.

Table S1: Surface density of $CTA^+$ and $Br^-$ and width of water-ion channels on different infinite polarizable gold surfaces. The standard error is given in small brackets.

| Exposed surface | $CTA^+/nm^2$ | $Br^-/nm^2$ | channel width [nm] |
|---|---|---|---|
| Au (111) | 1.30 (0.04) | 1.43 (0.06) | 0.68 (0.01) |
| Au(100) | 1.71 (0.01) | 1.65 (0.05) | 0.27 (0.01) |
| Au(110) | 1.67 (0.01) | 1.53 (0.05) | 0.36 (0.01) |

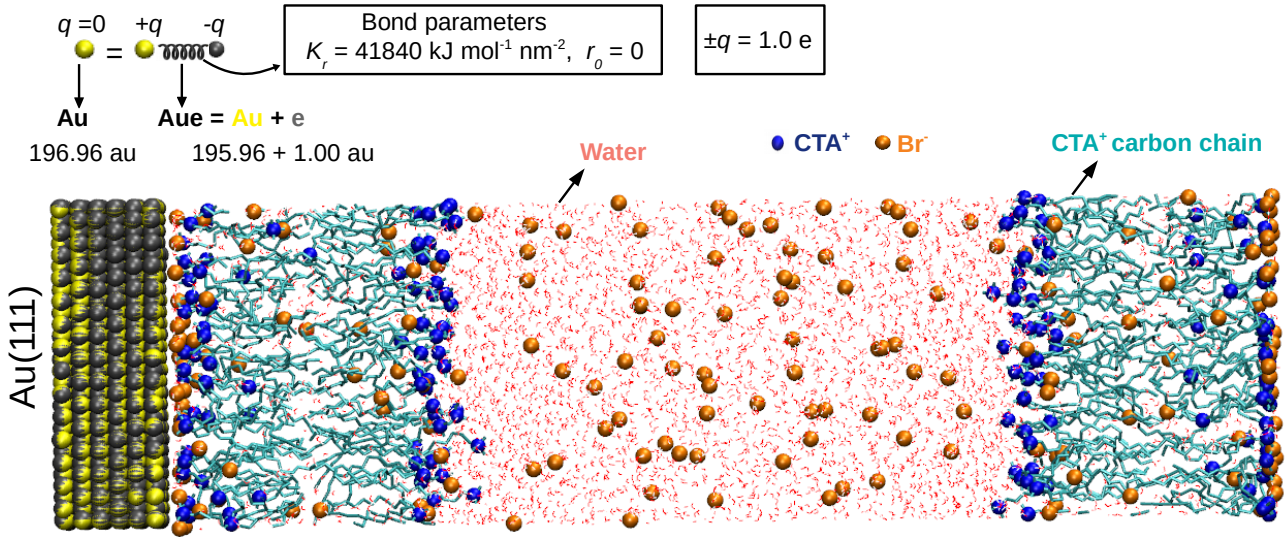


Figure S1: Initial configuration of the CTAB bilayer on Au(111) polarizable surface in water after energy minimization. After energy minimization, the system was first equilibrated in the NVT ensemble for 100 ps and NPT ensemble for 100 ps. Subsequently, a NPT ensemble production run MD simulations were performed for 500 ns.

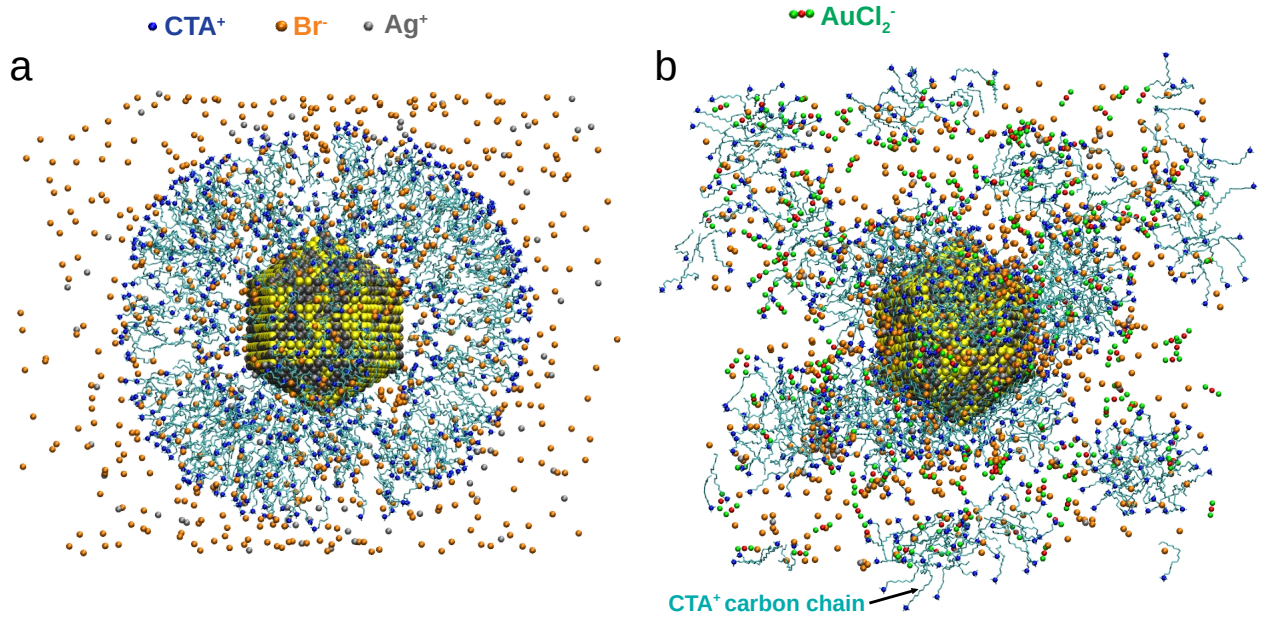


Figure S2: (a) Initial Configuration of the system without inclusion of $AuCl_2^-$:- Initial configuration of the CTAB bilayer around polarizable nanoseed including $Br^-$ and $Ag^+$ ions in water after energy minimization (Water molecules omitted for clarity). This system was production run for 555 ns. (b) Initial Configuration of the system with inclusion of $AuCl_2^-$:- $AuCl_2^-$ ions added in the final structure after 555 ns production run of the system without inclusion of $AuCl_2^-$. After addition of $AuCl_2^-$ ions this system was run for 771 ns.

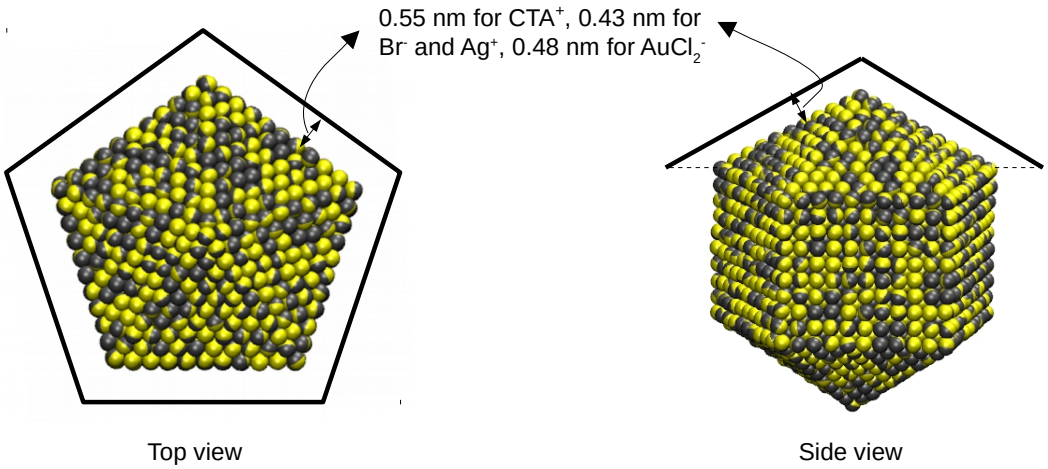


Figure S3: Top and side view of penta-twinned nanoseed with a representation of the cut-off for the surface density calculations.

Table S2: Surface density of $CTA^+$ and $Cl^-$ (cetyltrimethylammonium chloride, CTAC surfactant) on different infinite polarizable gold surfaces. The standard error is given in small brackets.

| Exposed surface | $CTA^+/nm^2$ | $Cl^-/nm^2$ |
|---|---|---|
| Au (111) | 0.72 (0.01) | 0.05 (0.05) |
| Au(100) | 0.59 (0.02) | 0.05 (0.04) |
| Au(110) | 0.96 (0.03) | 0.20 (0.09) |

# References

(1) Meena, S. K.; Sulpizi, M. Understanding the microscopic origin of gold nanoparticle anisotropic growth from molecular dynamics simulations. *Langmuir* **2013**, *29 (48)*, 14954–14961.

(2) Meena, S. K.; Sulpizi, M. From gold nanoseeds to nanorods: The microscopic origin of the anisotropic growth. *Angew. Chem. Int. Ed.* **2016**, *55 (39)*, 11960–11964.

(3) Meena, S. K.; Celiksoy, S.; Schafer, P.; Henkel, A.; Sonnichsen, C.; Sulpizi, M. The role of halide ions in the anisotropic growth of gold nanoparticles: a microscopic, atomistic perspective. *Phys. Chem. Chem. Phys.* **2016**, *18 (19)*, 13246–13254.

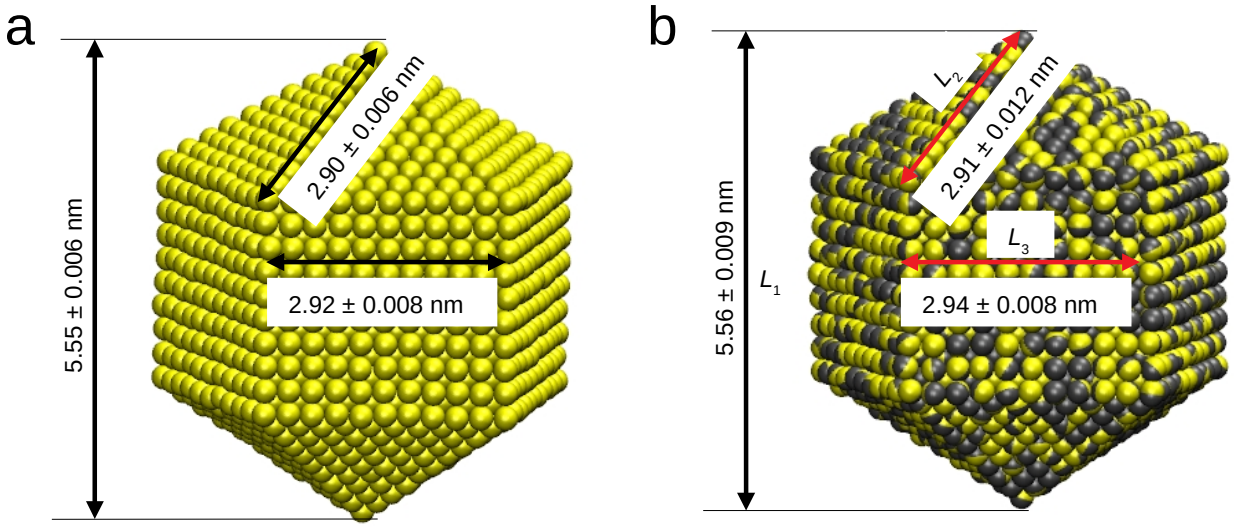


C

| Time (ns) | $L_1$ (nm) | $L_2$ (nm) | $L_3$ (nm) |
|---|---|---|---|
| 0 | 5.57 | 2.91 | 2.93 |
| 100 | 5.54 | 2.90 | 2.92 |
| 250 | 5.55 | 2.91 | 2.96 |
| 500 | 5.54 | 2.90 | 2.96 |

Figure S4: Gold nanoseed structure does not change due to inclusion of polarization effect, (a) non-polarizable nanosseed shown with dimension after 2950 ns from our previous work (Water molecules, $CTA^+$ and $Br^-$ are omitted for clarity).[2] Polarizable nanosseed is shown with dimensions after 771 ns from current work (Water molecules, $CTA^+$, $Br^-$, $Ag^+$ and $AuCl_2^-$ are not shown in the figure for clarity). The dimensions reported in the figure a and b are average from the last 50 ns. (c) The dimensions of polarizable nanoseed reported in table at different time.

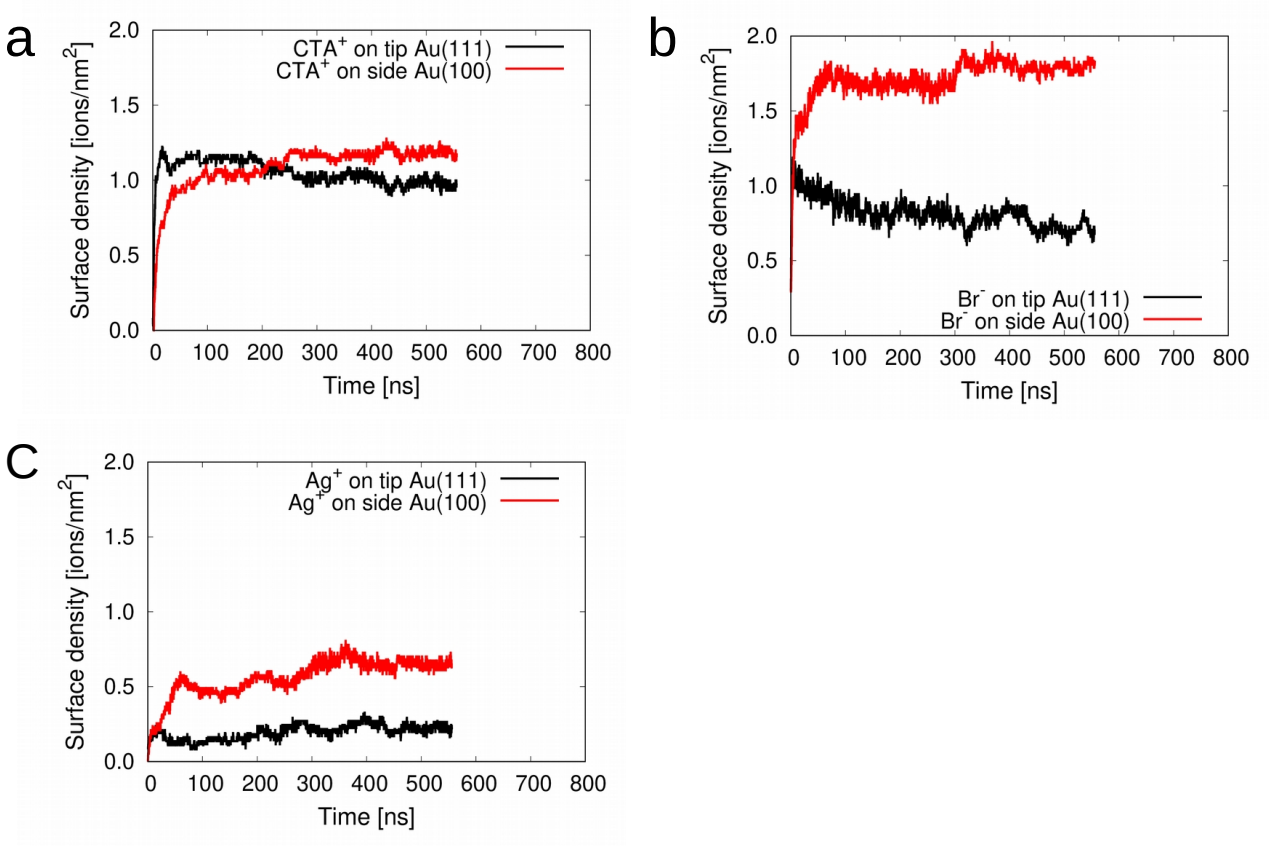


Figure S5: The surface densities of (a) $CTA^+$ (b) $Br^-$, and (c) $Ag^+$ are reported on the tip and side of polarizable nanosseed as a function of time for the system without inclusion of $AuCl_2^-$ (Figure2a and 2b in the main text). The average surface densities from last 100 ns are reported in Table S5.

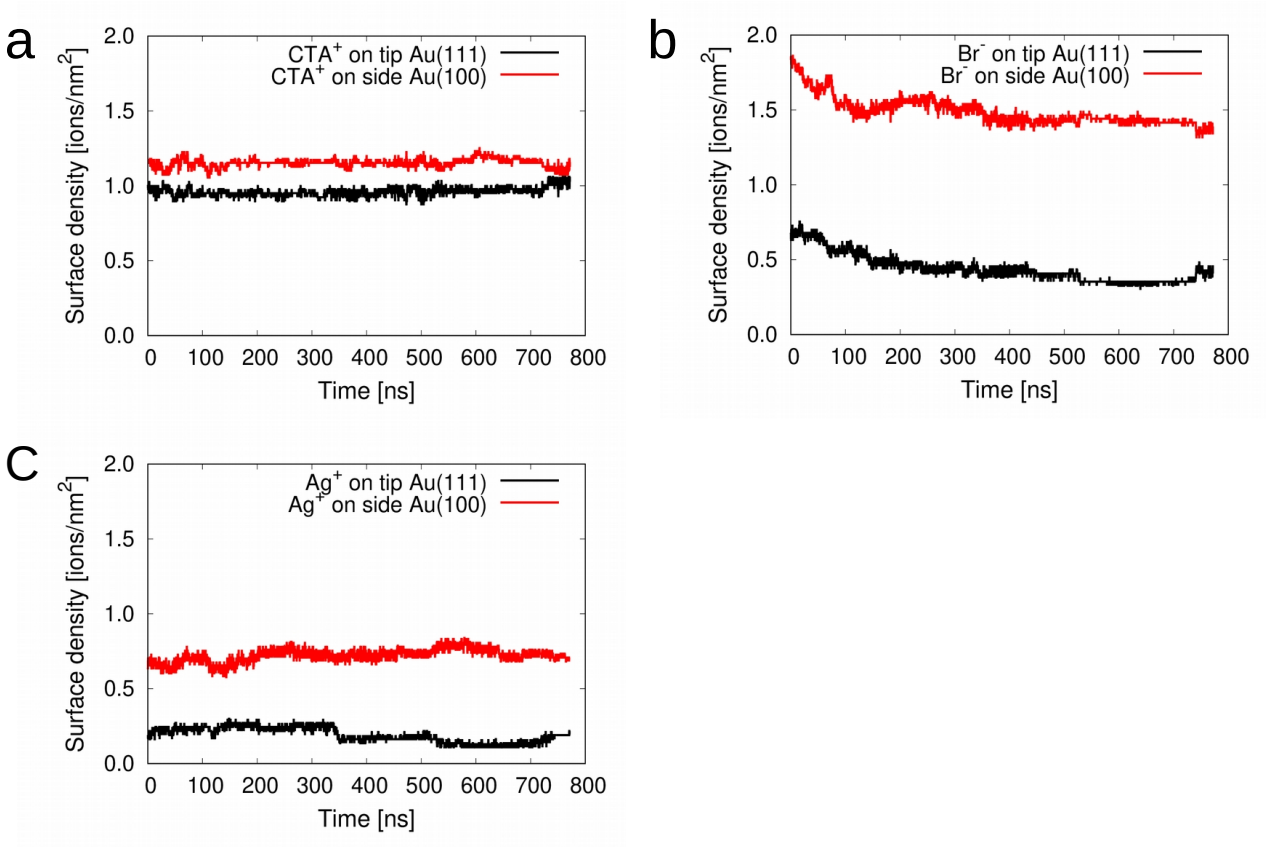


Figure S6: The surface densities of (a) $CTA^+$ (b) $Br^-$, and (c) $Ag^+$ are reported on the tip and side of polarizable nanosseed as a function of time for the system with inclusion of $AuCl_2^-$. The average surface densities from last 100 ns are reported in Table S6.

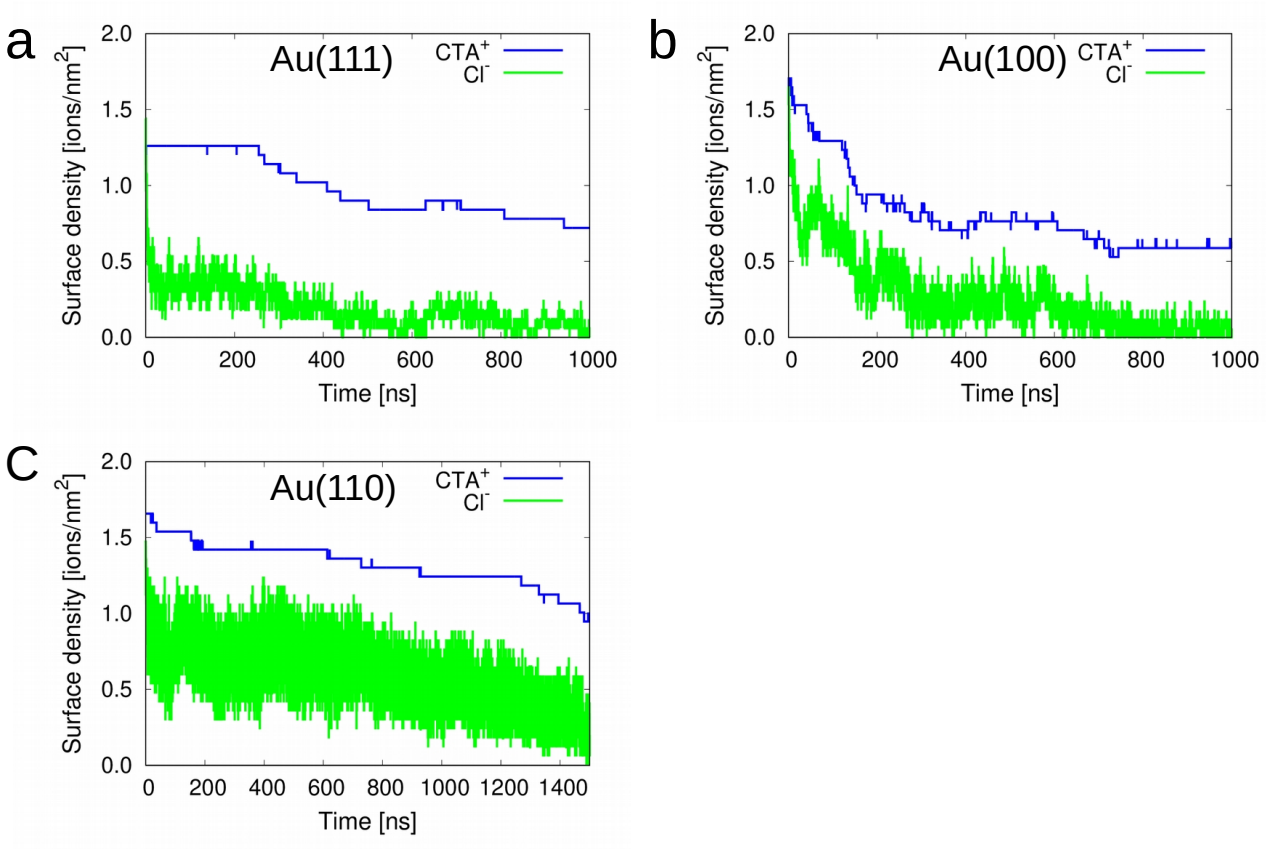


Figure S7: The surface densities of $CTA^+$ and $Cl^-$ on (a) Au(111), (b) Au(100) and (c) Au(110) are reported as a function of time. The average surface densities from last 100 ns are reported in Table S2.

Table S3: Surface density of $CTA^+$ and $I^-$ (cetyltrimethylammonium Iodide, CTAI surfactant) on different infinite polarizable gold surfaces. The standard error is given in small brackets.

| Exposed surface | $CTA^+/nm^2$ | $I^-/nm^2$ |
|---|---|---|
| Au (111) | 1.39 (0.02) | 1.46 (0.06) |
| Au(100) | 1.71 (0.01) | 1.75 (0.03) |
| Au(110) | 1.66 (0.01) | 1.60 (0.04) |

Table S4: Average thickness of CTAB, CTAC and CTAI surfactant layer on different gold surfaces. The maximum standard error in the layer thickness is 0.06 nm.

| Exposed surface | Au (111) | Au(100) | Au (110) (nm) |
|---|---|---|---|
| CTAB | 4.02 | 4.10 | 3.97 |
| CTAC | 1.87 | 1.82 | 1.99 |
| CTAI | 4.14 | 4.09 | 4.07 |

Table S5: Surface density of $CTA^+$, $Br^-$ and $Ag^+$ on different facets of polarizable nanoseed in the absence of reactant $AuCl_2^-$. The standard error is given in small brackets.

| | $CTA^+/nm^2$ | $Br^-/nm^2$ | $Ag^+$ |
|---|---|---|---|
| Au(111), tip | 0.98 (0.03) | 0.71 (0.04) | 0.22 (.02) |
| Au(100), side | 1.18 (0.03) | 1.79 (0.03) | 0.65 (.03) |

Table S6: Surface density of $CTA^+$, $Br^-$ and $Ag^+$ on different facets of polarizable nanograin in the presence of reactant $AuCl_2^-$. The standard error is given in small brackets.

| | $CTA^+/nm^2$ | $Br^-/nm^2$ | $Ag^+$ | $AuCl^{2-}$ |
|---|---|---|---|---|
| Au(111), tip | 0.99 (0.04) | 0.38 (0.04) | 0.16 (.03) | 0.71 (.04) |
| Au(100), side | 1.14 (0.03) | 1.40 (0.03) | 0.72 (.02) | 0.53 (.03) |

Table S7: The equilibrium surface density, $\rho_e$ and adsorption coefficient, $k$ from model fitting to surface density variation with time on the tip and the side.

| | equilibrium surface density, $\rho_e$ [ions/nm$^2$] | adsorption coefficient, $k$ [nm$^2$/(ions.t)] |
|---|---|---|
| Au(111), tip | 0.7738 | 0.0167 |
| Au(100), side | 0.6784 | 0.0081 |